Applied Physics A (2023) 129:774
https://doi.org/10.1007/s00339-023-07047-5

Applied Physics A
Materials Science & Processing

Elimination of trap density by NH_4Cl passivation for high-performance perovskite solar cells

Qianliu Yin[1] · Fanfan Zhang[2] · Yanlin Teng[3] · Cong Peng[3] · Chaonan Wang[3] · Yonglong Jin[3] · Meifeng Xu[3] · Tian Xu[3]

Received: 30 June 2023 / Accepted: 2 October 2023 / Published online: 17 October 2023

Abstract
Different concentrations of NH_4Cl are introduced to $MAPbI_3$ precursor solution, planar $MAPbI_3$ perovskite films, and solar cells' performance with or without NH_4Cl have been studied. The $NH_4Cl/MAPbI_3$ films exhibit increased grain size and narrowed grain boundaries. The light absorption of perovskite films with different concentrations of NH_4Cl was also evaluated. To understand the growth of perovskite films with NH_4Cl added to perovskite precursor solutions, XRD and XPS spectroscopy were conducted on different perovskite film samples. By adding NH_4Cl, the $MAPbI_3$ film shows good crystal quality and the shift of Pb peaks indicates that NH_4Cl is not physically mixed but chemically incorporated into $MAPbI_3$ films. We attribute the effect to Cl ions of NH_4Cl combining with free lead ions of $MAPbI_3$ so as to fill the vacancy of volatile I ions in the NH_4Cl–$MAPbI_3$ films. The 20 mg NH_4Cl-based device showed an enhanced performance of a PCE of 13.67% compared to the device without adding NH_4Cl with a PCE of 10.24%. The introduction of 20 mg NH_4Cl achieved the best passivation effect. Using a 20 mg NH_4Cl device, the trap density can be reduced to 0.84×10^{16} cm^{-3}, resulting in more efficient charge removal from the surface and improved performance.

Keywords NH_4Cl · Passivation · Defect · Perovskite

1 Introduction

In the past few decades, organic and inorganic hybrid perovskite have attracted more and more attention due to their superior photoelectric properties [1–4]. The power conversion efficiency (PCE) of single-junction perovskite solar cells has recently increased from 3.8% to more than 25% [5–8]. Inverted perovskite solar cells offer high stability, low hysteresis, and lightweight characteristics, making them suitable for great application in wearable electronic devices and tandem perovskite solar cells [9–11]. However, the PCE of inverted perovskite solar cells has been lower than that of regular perovskite solar cells resulting from the perovskite film serious recombination loss [12, 13]. A large number of traps on the grain boundary of perovskite films hinder carrier separation and lead to charge non-radiative recombination, which is an important reason for the low performance of inverted perovskite solar cells [14, 15]. Therefore, improving the quality of the perovskite film is very important for the efficiency and stability of inverted perovskite solar cells. A simple and effective method to increase the grain sizes of perovskite films is urgently needed. Furthermore, passivation strategies were confirmed as an efficient method of suppressing perovskite film defects [16–18].

In the process of preparation of perovskite films, improving the quality of perovskite films by adding additives with specific functional groups is widely discussed. The addition of specific functional groups can effectively passivate the defects in the perovskite matrix, such as amine ($–NH_2$), hydroxyl (–OH), acid ($–SO_3$), or halides, can effectively passivate the defects in the perovskite matrix, and improve the quality and optoelectronic properties of the films [19–23]. When Cl^- is added to iodized perovskites, it can replace iodine, reduce the number of iodine vacancies, achieve better crystallization quality, and improve the stability of the

✉ Meifeng Xu
mfxu@ntu.edu.cn

✉ Tian Xu
xutian@ntu.edu.cn

[1] First unit, Nantong University, Nantong 226019, Jiangsu, China

[2] Second unit, Qidong Middle School, Qidong, Nantong 226299, Jiangsu, China

[3] Nantong University, Nantong 226019, Jiangsu, China

material [24]. It has been found that the addition of ammonium cation (NH_4^+) into organic perovskites can regulate and optimize the microstructure of the perovskite film, which in turn enhances its performance. In addition, NH_4^+ cations could properly fill into the vacancies of MA, or enter into the interstitial places of MA to passivate defects. The NH_4^+ cation compared to the Na^+ or K^+ due to its larger ion radius, and the cation with a larger ionic radius makes it more difficult to enter the MA ionic gap, thus reducing the defects caused by the addition of too much non-perovskite phase to the perovskite film, which can better passivate the trap states in perovskite [25, 26].

In this manuscript, ammonium chloride (NH_4Cl) is introduced into a perovskite precursor solution to optimize the properties of perovskite films. For comparison, NH_4Cl-free inverse structures were also prepared under the same fabrication conditions. With the addition of NH_4Cl, the crystallites of perovskite films were enhanced and grain boundaries were reduced. X-ray photoelectron spectroscopy (XPS) was used to detect the effect of NH_4Cl on perovskite films. These results show that 20 mg NH_4Cl effectively passivates perovskite films, and the density of trap states was reduced. Compared with the pure perovskite device with a PCE of 10.24%, the efficiency of the perovskite solar cell based on 20 mg NH_4Cl reaches 13.67%. Our results provide a surface treatment method for the inverted perovskite solar cells that can deliver high-efficiency outcomes. This strategy offers the obvious potential for perovskite-based photovoltaic technologies and greatly promotes their development. For another, larger perovskite grains have a superior photoelectric response, making them ideal for use in photoconductive detectors and photosensitive sensors. In addition, the process of passivating perovskites has several benefits, including efficient electron–hole pair separation, faster charge migration, and higher stability. These advantages are of great significance in the field of photocatalysis and photovoltaic power generation and are a great progress in the development of clean energy [27].

2 Experimental section

2.1 Experiment materials

Lead iodide (PbI_2, Aladdin, 99.9%), methylammonium iodide (CH_3NH_3I, Macklin, 99.5%), dimethyl sulfoxide (DMSO, Aladdin, 99.9%), γ-butyrolactone (GBL, J&K Scientific Ltd, 99%), 3,4-oxyethyleneoxythiophene-poly (styrene sulfonate) (PEDOT:PSS, J&K Scientific Ltd.), [6,6]-phenyl-C61-butyric acid methyl ester (PCBM, Bide medicine, 99.7%), chlorobenzene(C_6H_5Cl, J&K Scientific Ltd. 98.0%), anhydrous ethanol(C_2H_6O, Lingfeng, 99.7%), bathocuproine (BCP, Baolaite, 99%), and ammonium chloride(NH_4Cl, 99.5%).

2.2 Device fabrication

ITO glass is cleaned with ethanol and acetone for 30 min to remove the pollutants from the glass surface and irradiated with ultraviolet to change its hydrophobicity. The ITO glass was then placed in a spin coater. 80 µL PEDOT:PSS is spin-coated on the ITO at 4000 rpm for 30 s, then annealed at 110 ℃ for 30 min. Next, 50 µL $CH_3NH_3PbI_3$ precursor solution (470.9 mg PbI_2, 162.4 mg MAI in a mixture of 0.7 mL GBL and 0.3 mL DMSO) was spin-coated on the PEDOT:PSS layer at 1500 rpm for 20 s and 4000 rpm for 40 s, then annealed at 110 °C for 10 min. 50 µL PCBM spin-coated on the $CH_3NH_3PbI_3$ layer at 2000 rpm for 30 s, then annealed at 90 °C for 10 min. 50 µL BCP spin-coated on the PCBM layer at 2000 rpm for 20 s, then annealed at 80 °C for 10 min. PCBM is considered an electron transport layer (ETL), and BCP promotes the charge transfer between the ETL and Ag electrode. Finally, the 100 nm Ag stick electrode was evaporated on the BCP layer by using vacuum evaporation coating technology (vacuum is 8.0×10^{-4} pa, film deposition rate is 0.2 Å/s).

$CH_3NH_3PbI_3$ with NH_4Cl: 10 mg, 20 mg, and 30 mg NH_4Cl were added to 1 ml of the perovskite precursor solution.

2.3 Characterization methods

The surface morphology and the crystallinity of perovskite films were characterized by scanning electron microscopy (SEM, Gemini-300, Carl Zeiss, Germany). The crystallinity of perovskite was measured by X-ray diffraction technique (XRD, Rigaku Ultima IV, Japan). The absorption spectra of perovskite films were conducted on a UV/vis spectrophotometer (UV-1800, Shimadzu). Raman spectroscopy used for detection is Advantage NIR spectrometer, Deltanu. Elemental analysis of perovskite films with ammonium chloride was carried out by X-ray photoelectron spectrometer (XPS, K-Alpha+, America). The excitation source was the monochromatic Al Kα X-ray beam operated at 72 W, and the electron emission angle was 0°. The energy step was 0.05 eV for detail spectra and 1 eV for survey spectra. The size of the analyzed sample area was 400 µm. The sample wasn't cleaned with Ar^+ ion sputtering before XPS measurement and we don't use charge neutralizer in our operation. The performance of PSCs was assessed by a photovoltaic system (AM 1.5 G, 100 mW/cm2, Growntech. INC, IV Test Station 2000 AAA).

3 Results and discussion

The cuboid growth of $MAPbI_3$ here can be optimized by adjusting the NH_4Cl concentration in perovskite precursors, as can be observed by scanning electron microscopy (SEM). As shown in Fig. 1(a), the size of the neat $MAPbI_3$ perovskite film crystal is smaller and the surface is relatively smooth. With 10 mg NH_4Cl added to the $MAPbI_3$ precursor solution, the morphology of the perovskite film changes in Fig. 1(b), and the grain size tends to increase. After 20 mg NH_4Cl is added, the crystal size further increases and the gap between the grain boundaries narrows (Fig. 1(c)). Increased crystal size and narrowed grain boundaries are conducive to reducing defects of the perovskite films, which will be discussed later. Figure 1(d) shows that the crystal size increases a lot by adding 30 mg NH_4Cl to the $MAPbI_3$ precursor solution, but the aggregation of grains also leads to large gaps, which causes direct contact between ETL and the hole transport layer (HTL). In the experiment, the $MAPbI_3$ precursor solution close to saturation, and even some turbid precipitation appearing, indicate that the passivation effect of NH_4Cl has reached the limit.

The light absorption of perovskite films with different concentrations of NH_4Cl was also evaluated by a UV–Vis spectrophotometer. Neat perovskite has a wide range of light absorption, and it also shows a strong absorption around 750 nm [28]. From Fig. 1(e), perovskite exhibits different light absorption after the addition of NH_4Cl in the wavelength range of 600 nm to 800 nm. The absorption of perovskite films is enhanced after the addition of NH_4Cl, which is due to the larger grain sizes of the $MAPbI_3$ film. The greater the crystal size and narrower the grain boundaries with 20 mg NH_4Cl, the more effectively it can absorb light. Because of the influence of the high-angle boundary with 30 mg NH_4Cl, the surface morphology of the film is damaged, and the absorption of perovskite film also weakens.

To understand the growth of perovskite films with NH_4Cl added to perovskite precursor solutions, XRD (X-ray diffraction) is conducted on different perovskite film samples. As shown in Fig. 1f, the diffraction peak angles of $MAPbI_3$ are located at 14.1°, 28.4°, and 31.8°, corresponding to the (110), (220), and (310) planes of perovskite crystal structure [29, 30]. The weak PbI_2 peaks (12.8°) indicate that PbI_2 is almost completely transformed into $MAPbI_3$. By comparing the diffraction peak intensity of perovskite crystals, it is found that the crystal quality of $MAPbI_3$ film improves well after adding NH_4Cl, and the effect was the best for adding 20 mg NH_4Cl. The addition of 30 mg NH_4Cl to $MAPbI_3$ films causes a weakening of their diffraction peak, suggesting that an increase in NH_4Cl occurrence negatively affects the film. These results are consistent with SEM morphology and absorption data.

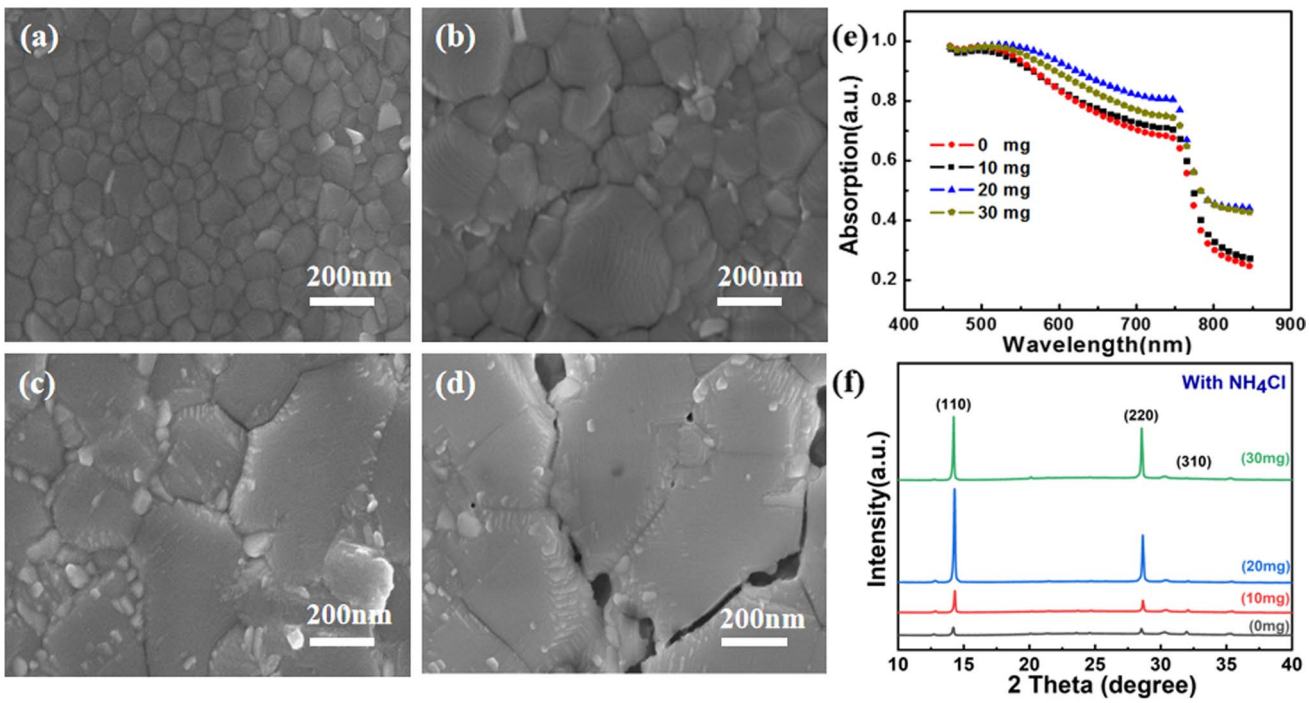

Fig. 1 SEM images of the perovskite films without (**a**) or with different concentrations (10 mg (**b**), 20 mg (**c**), 30 mg (**d**)) of NH_4Cl to perovskite precursor solution, (**e**) Absorption and (**f**) XRD spectroscopy of the perovskite films with or without NH_4Cl

Furthermore, we study the reasons why adding NH_4Cl improved the characteristics of $MAPbI_3$ films. From Fig. 2a, the Pb 4f XPS spectra show that the Pb 4f peaks for perovskite films with 20 mg NH_4Cl shift toward a higher binding energy compared to neat $MAPbI_3$ film. The shift of Pb peaks indicates that NH_4Cl is not only physically mixed but chemically incorporated into $MAPbI_3$ films, and we suppose the I-Pb-Cl structure is likely formed in the NH_4Cl–$MAPbI_3$ films. To validate our hypothesis, we examine the XPS spectra of other elements. As shown in Fig. 2b, c, I 3d and N 1s characteristic peaks show some displacement of binding energy, which is attributed to the combination of Pb–Cl. Cl 3d characteristic peaks are also shown in Fig. 2d, which indicates that NH_4Cl has been successfully combined with $MAPbI_3$ films. It can be seen that 20 mg NH_4Cl combined with $MAPbI_3$ film has the maximal relative content of Cl, which means that more Cl ions remain in the perovskite and bind with free Pb ions. Cl ions are combined with free Pb ions to fill the vacancy of volatile I ions, indicating that NH_4Cl has a passivation effect on $MAPbI_3$ films. The added NH_4Cl effectively passivates the grain boundary defects of perovskite to promote the nucleation and crystal growth of the $MAPbI_3$ film, and fully covers the substrate to obtain high-quality perovskite films, which helps improve the performance of perovskite solar cells.

To estimate the photovoltaic performance enhanced with NH_4Cl added by increasing the light absorption and larger crystal size and narrowed grain boundaries. We fabricated inverted perovskite solar cells with the structure of ITO/PEDOT:PSS/$MAPbI_3$ (with or without NH_4Cl)/PCBM/BCP/Ag.

The current density and voltage of different devices are shown in Fig. 3a, and their corresponding parameters are listed in Table 1. The device without adding NH_4Cl exhibits a PCE of 10.24%, with an open-circuit voltage (V_{oc}) of 0.87 V, a short-circuit current density (J_{sc}) of 17.06 mA/cm^2 and 68.89% fill factor (FF). The small values of these parameters are mainly the result of the recombination caused by defects in perovskite solar cells. The more grain boundaries, the more energy loss, the faster the decay of charge carriers, and the lower the charge transfer efficiency. After adding NH_4Cl to the perovskite precursor solution, the device performance improves, so these results indicate that the NH_4Cl is an effective passivation for the perovskite defects.

After adding 10 mg NH_4Cl, the PCE of the device increases to 12.31%, and, FF also greatly improves, indicating that the device defects are reduced by NH_4Cl. Device PCE reaches the best value of 13.67% when adding 20 mg NH_4Cl, indicating that the introduction of 20 mg NH_4Cl achieves the best passivation effect. The improved V_{oc} and FF values result from the effective passivation of NH_4Cl, and the enhancement is attributed to the good crystallization of NH_4Cl–$MAPbI_3$ films. The neat perovskite device and best device hysteresis have also been studied, as shown in Fig. 3b, c. These two devices present no obvious hysteresis. The device parameters of 30 mg NH_4Cl once again prove

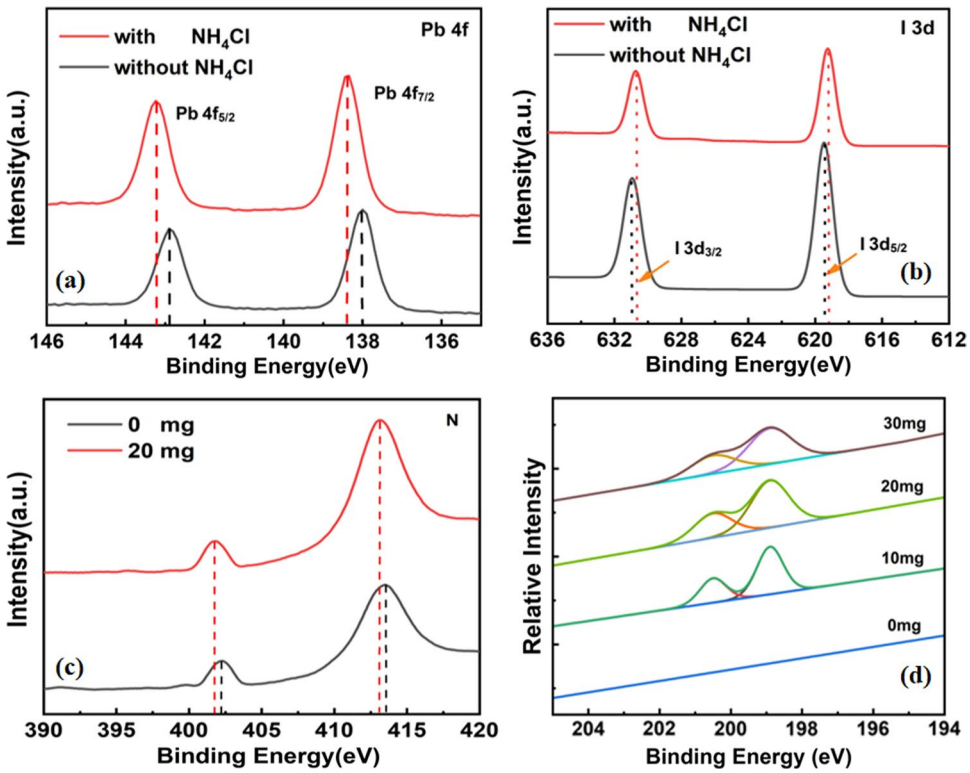

Fig. 2 (**a**) XPS spectra of Pb 4f, (**b**) I 3d and (**c**) N 1s characteristic peaks without or with 20 mg NH_4Cl. (**d**) Cl 3d characteristic peaks without or with different NH_4Cl concentrations

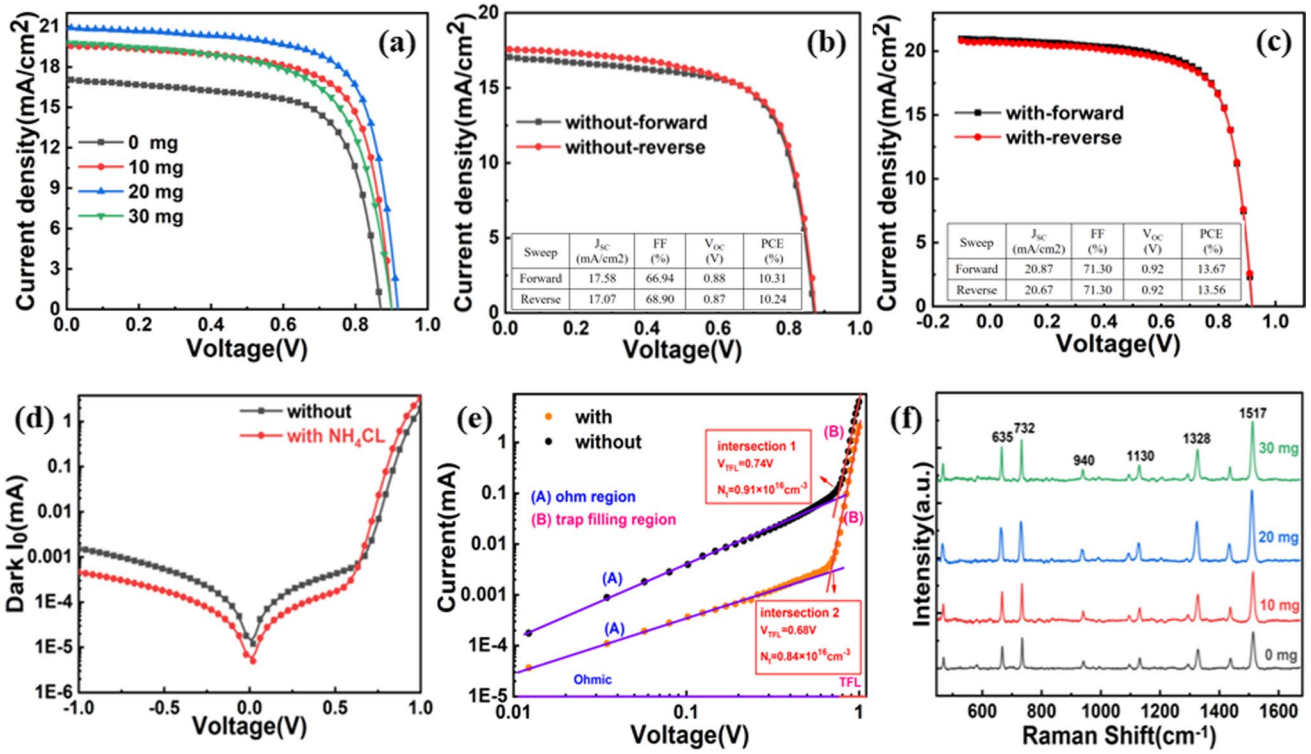

Fig. 3 (**a**) The current density and voltage curves of different NH_4Cl-based devices. Forward and reverse scan directions without (**b**) or with (**c**) 20 mg NH_4Cl-based devices. The neat perovskite device and 20 mg NH_4Cl-based devices' dark current density (**d**) and trap state density (**e**). (**f**) Raman spectroscopy of CuPc on perovskite films with or without NH_4Cl

Table 1 *J–V* characteristics parameters of devices with different NH_4Cl concentrations and without the NH_4Cl on the perovskite layers

Devices	V_{oc} (V)	J_{sc} (mA/cm^2)	FF (%)	PCE (%)
0	0.87	17.06	68.89	10.24
10	0.90	19.61	69.64	12.31
20	0.92	20.87	71.30	13.67
30	0.90	19.81	64.98	11.60

that excessive NH_4Cl addition will destroy the photoelectric properties of $MAPbI_3$ films.

To investigate the defect passivation effect in detail, we measured the neat perovskite device and the best device dark current density and trap density of state. In this work, both devices have good diode properties and can provide good photocurrent (Fig. 3d). The utilization of a 20 mg NH_4Cl-based device results in a dark current reduction, which means less current leakage, helps to reduce the shunt resistance of the device and facilitates charge transfers (CT) between interface layers, thus enabling the device to show higher conversion efficiency.

To calculate the trap state of the device with or without 20 mg NH_4Cl, hole-only devices are equipped with a structure of ITO/PEDOT:PSS/Perovskite/MoO_3/Au. According to the space charge limited current (SCLC) model, the start of the trap filling limit voltage (V_{TFL}) of the device with 20 mg NH_4Cl added shows a relatively low value of 0.68 V (Fig. 3e), whereas 0.74 V V_{TFL} is obtained for the device without passivation treatment. Using the following formula between V_{TFL} and defect state density (N_t):

$$N_t = \frac{2\varepsilon_0 \varepsilon V_{TFL}}{eL^2}.$$

e is the basic charge, L is the thickness of perovskite layers, ε is the relative dielectric constant of perovskite films, ε_0 is the permittivity of vacuum. According to the values of V_{TFL}, the N_t of the neat perovskite device is calculated with a value of 0.91×10^{16} cm^{-3}, and the N_t of 20 mg NH_4Cl-based device decreases to 0.84×10^{16} cm^{-3}. Reduced trap density leads to efficient charge extraction from the surface, which limits V_{oc} losses and improves FF, and this is consistent with current density and voltage results. This also proves that NH_4Cl can effectively passivate perovskite film defects.

To further study the interaction between NH_4Cl and perovskite films, Raman spectroscopy is used to study the properties of perovskite films. From Fig. 3f, a CuPc solution with a concentration of 1×10^{-3} M is deposited on perovskite films with or without NH_4Cl, and then quickly

dried in a nitrogen glove box. The Raman spectral integration time is set to 5 s with a resolution of 2 cm^{-1}. The characteristic peaks of CuPc appear at 635 cm^{-1}, 732 cm^{-1}, 1130 cm^{-1}, 1328 cm^{-1}, and 1517 cm^{-1}, respectively. Among them, the film with the strongest characteristic peak for 20 mg NH_4Cl, indicates that the degree of passivation of $MAPbI_3$ film is the highest at this time, and the filling of inherent defects enhances charge transfers, which is consistent with our previous research results.

4 Conclusion

We have shown an efficient way to passivate perovskite films by inserting different concentrations of NH_4Cl into the $MAPbI_3$ precursor solution. The defects of NH_4Cl passivated perovskite films result in larger grains and fewer grain boundaries, thus enhancing the electron–hole transport rate. The larger crystal size and narrowed grain boundaries with NH_4Cl lead to a better increase in their absorption. The $MAPbI_3$ film exhibits optimal crystal structure when 20 mg of NH_4Cl is added to the SEM morphology and absorption data. The reason why adding NH_4Cl improved the characteristics of $MAPbI_3$ films is that Cl ions combine with free lead ions so as to fill the vacancy of volatile I ions. The best device PCE obtained a value of 13.67% when adding 20 mg NH_4Cl, indicating that the introduction of 20 mg NH_4Cl achieved the best passivation effect and showed lower trap density with a value of 0.84×10^{16} cm^{-3}.

Acknowledgements We acknowledge the financial support from the National Natural Science Foundation of China (NSFC) (*Nos.* 61701261), the Natural Science Foundation of Jiangsu Province (*Nos.* BK20160417) and the Innovation and Entrepreneurship Training program for College students in Jiangsu Province of China (*Nos.* 202310304004Z).

Author contributions QY: Investigation, Methodology, Writing—original draft. FZ: Investigation, Writing. YT: Conceptualization. CP: Visualization. CW: Review. YJ: Review. MX: Writing—review and editing. TX: Review and Supervision.

Data availability Data will be made available on request.

Declarations

Conflict of interest The authors declare that they have no known competing financial interests or personal relationships that could have appeared to influence the work reported in this paper.

Ethical approval The authors declare that this manuscript is original, has not been published before, and is not currently being considered for publication elsewhere. This submission in its present form is approved by all authors.

References

1. M. Chen, Y. Tang, R. Qin, Z. Su, F. Yang, C. Qin, J. Yang, X. Tang, M. Li, H. Liu, Perylene Monoimide Phosphorus Salt Interfacial Modified Crystallization for Highly Efficient and Stable Perovskite Solar Cells. ACS applied materials & interfaces. 15, 5556–5565, (2023).https://doi.org/10.1007/s11082-020-02342-4
2. S. Wang, Perovskite Tandem Solar Cell Technologies. Energies. 16, 1–3, (2023).https://www.mdpi.com/1996-1073/16/4/1586/
3. A.M. Elseman, M.M. Rashad, Influence of nitrogen atmosphere one-step heating assisted the solution processing of Kesterite Cu_2ZnSnS_4 as hole extraction on the efficacy of the inverted perovskite solar cells. Optical Materials. 124, 111998, (2022).https://doi.org/10.1016/j.optmat.2022.111998
4. P.M. Sonar, H.D. Pham, X. Li, W. Li, S. Manzhos, A.K.K. Kyaw, Organic Interfacial Materials for Perovskite-based Optoelectronic Devices. Energy & Environmental Science. 12, 1177–1209, (2019).https://doi.org/10.1039/C8EE02744G
5. L. Lin, P. Li, L. Jiang, Z. Kang, Q. Yan, H. Xiong, S. Lien, P. Zhang, Y. Qiu, Boosting efficiency up to 25% for HTL-free carbon-based perovskite solar cells by gradient doping using SCAPS simulation. Solar Energy. 215, 328–334, (2021).https://doi.org/10.1016/j.solener.2020.12.059
6. Z. Djuri, I. Joki, Ideal efficiency of resonant cavity-enhanced perovskite solar cells. Optical and Quantum Electronics. 52, 230, (2020).https://doi.org/10.1007/s11082-020-02342-4
7. N.K. Tailor, M. Abdi-Jalebi, V. Gupta, H. Hu, M.I. Dar, G. Li, S. Satapathi, Recent progress in morphology optimization in perovskite solar cell. Journal of Materials Chemistry A. 8, 21356–21386, (2020).https://doi.org/10.1039/D0TA00143K
8. G. Jang, H. Han, S. Ma, J. Lee, C.U. Lee, W. Jeong, J. Son, D. Cho, J.H. Kim, C. Park, Rapid crystallization-driven high-efficiency phase-pure deep-blue Ruddlesden–Popper perovskite light-emitting diodes. Advanced Photonics. 5, 016001, (2023).https://doi.org/10.1117/1.AP.5.1.016001
9. C.H. Chiang, M.K. Nazeeruddin, M. Gratzel, C.G. Wu, The synergistic effect of H_2O and DMF towards stable and 20% efficiency inverted perovskite solar cells. Energy & Environmental Science. 10, 808–817, (2017).https://doi.org/10.1039/C6EE03586H
10. M. Loizos, M. Tountas, N. Tzoganakis, C.L. Chochos, A. Nega, A. Schiza, C. Polyzoidis, V.G. Gregoriou, E. Kymakis, Enhancing the lifetime of inverted perovskite solar cells using a new hydrophobic hole transport material. Energy Advances. 1, 312–320, (2022).https://doi.org/10.1039/D2YA00067A
11. X. Yuan, H. Li, J. Fan, L. Zhang, F. Ran, M. Feng, P. Li, W. Kong, S. Chen, Z. Zang, Enhanced p-Type Conductivity of NiOx Films with Divalent Cd Ion Doping for Efficient Inverted Perovskite Solar Cells. ACS applied materials & interfaces. 14, 17434–17443, (2022).https://doi.org/10.1021/acsami.2c01813
12. Y. Zhu, S. Wang, R. Ma, C. Wang, The improvement of inverted perovskite solar cells by the introduction of CTAB into PEDOT:PSS. Solar Energy. 188, 28–34, (2019).https://doi.org/10.1016/j.solener.2019.05.073
13. Q.B. Ke, J.R. Wu, C.C. Lin, S.H. Chang, Understanding the PEDOT:PSS, PTAA and P3CT-X Hole-Transport-Layer-Based Inverted Perovskite Solar Cells. Polymers. 14, 823, (2022).https://doi.org/10.3390/polym14040823
14. Z. Wang, J. Tao, J. Shen, W. Kong, Z. Yu, A. Wang, G. Fu, S. Yang, Multifunctional molecular incorporation boosting the efficiency and stability of the inverted perovskite solar cells. Journal of Power Sources. 488, 229449, (2021).https://doi.org/10.1016/j.jpowsour.2021.229449
15. S. Asgharizadeh, S.K. Azadi, M. Lazemi, Understanding the pathways toward improved efficiency in MXene-assisted

perovskite solar cells. Journal of Materials Chemistry C. 10, 1776–1786, (2022).https://doi.org/10.1039/D1TC04643H
16. F. Gao, Y. Zhao, X. Zhang, J. You, Recent Progresses on Defect Passivation toward Efficient Perovskite Solar Cells. Advanced Energy Materials. 10, 1902650, (2020).https://doi.org/10.1002/aenm.201902650
17. W. Wanhai, Z. Jie, T. Weihua, Passivation Strategies of Perovskite Film Defects for Solar Cells. J. Inorg. Mater. 37, 129–139 (2022).https://doi.org/10.15541/jim20210117
18. R. Zhao, L. Xie, R. Zhuang, T. Wu, R. Zhao, L. Wang, L. Sun, Y. Hua, Interfacial Defect Passivation and Charge Carrier Management for Efficient Perovskite Solar Cells via a Highly Crystalline Small Molecule. ACS Energy Lett. 6, 4209–4219 (2021).https://doi.org/10.1021/acsenergylett.1c01898
19. Z. Yang, J. Dou, S. Kou, J. Dang, Y. Ji, G. Yang, W.Q. Wu, D.B. Kuang, M. Wang, Multifunctional Phosphorus-Containing Lewis Acid and Base Passivation Enabling Efficient and Moisture-Stable Perovskite Solar Cells. Advanced Functional Materials. 30, 1910710, (2020).https://doi.org/10.1002/adfm.201910710
20. K. Tang, S. Xie, G.R. Cofield, X. Yang, E. Tian, H. Lin, Catalytic transfer hydrogenation of furfural for the production of ethyl levulinate: Interplay of Lewis and Bronsted acidities. Energy Technol. 6, 1826–1831 (2018).https://doi.org/10.1002/ente.201700973
21. J. Xie, Z. Zhou, H. Qiao, M. Chen, L. Wang, S. Yang, Y. Hou, H. Yang, Modulating $MAPbI_3$ perovskite solar cells by amide molecules: Crystallographic regulation and surface passivation. J Energy Chem. 56, 179–185, (2021).https://doi.org/10.1016/j.jechem.2020.07.050
22. J.S. Benas, F.C. Liang, W.C. Chen, Lewis adduct approach for self-assembled block copolymer perovskite quantum dots composite toward optoelectronic application: Challenges and prospects. Chemical Engineering Journal. 431, 133701, (2022).https://doi.org/10.1016/j.cej.2021.133701
23. Q. Yang, X. C. Wang, S. W. Yu, X. Liu, P. Gao, X. B. Hu, G. J. Hou, S. Q. Chen, X. Guo, C. Li, Solvent-Actuated Self-Assembly of Amphiphilic Hole-Transporting Polymer Enables Bottom-Surface Passivation of Perovskite Film for Efficient Photovoltaics. Advanced Energy Materials. 11(17), 2100493, (2021). https://doi.org/10.1002/aenm.202100493
24. A. Wincukiewicz, J.B. Jasinski, M. Tokarczyk, R. Pietruszka, M. Kaminska, The effects of doping and coating on degradation kinetics in perovskites. Solar Energy Materials and Solar Cells. 230, 111142, (2021).https://doi.org/10.1016/j.solmat.2021.111142
25. S. R. Pathipati, M. N. Shah, Performance enhancement of perovskite solar cells using NH_4I additive in a solution processing method. Solar Energy, 162(3), (2018).https://doi.org/10.1016/j.solener.2017.12.043
26. G. F. Han, Hadi, et al. Additive Selection Strategy for High Performance Perovskite Photovoltaics.The journal of physical chemistry, C. Nanomaterials and interfaces, 122(25), 13884–13893, (2018). https://doi.org/10.1021/acs.jpcc.8b00980
27. P. Chen, W.J. Ong, Z. Shi, X. Zhao, N. Li, Pb-based halide perovskites: recent advances in photo (electro) catalytic applications and looking beyond. Adv. Func. Mater. **30**, 1909667 (2020). https://doi.org/10.1002/adfm.201909667P
28. K.A. Parrey, S.G. Ansari, A. Aziz, A. Niazi, Enhancement in structural and optical properties of Cd doped hybrid organic-inorganic halide perovskite $CH_3NH_3Pb_{1-x}Cd_xI_3$ photo-absorber - ScienceDirect. Materials Chemistry and Physics. 241, 122387, (2020).https://doi.org/10.1016/j.matchemphys.2019.122387
29. W.W. Lin, J.R. Wu, Y. Nakanishi, L.C. Chen, Investigation on optoelectronic characteristics of porous silicon/TiO_2/$CH_3NH_3PbI_3$/graphene heterostructure light-emitting diodes prepared by spin-coating. Spie Nanoscience + Engineering.9558, 95580M, (2015).https://doi.org/10.1117/12.2187890
30. X. Wang, H. Sarvari, H. Dang, V. Singh, Z. Chen, Preparation and evaluation of perovskite solar cells in the absolute atmospheric environment. Spie/cos Photonics Asia. 10019, 100190B, (2016).https://doi.org/10.1117/12.2247659